Title

Guanidinylated Neomycin Conjugation Enhances Intranasal Enzyme Replacement in the Brain

Journal

Molecular Therapy, 25(12)

ISSN

1525-0016

Authors

Tong, Wenyong
Dwyer, Chrissa A
Thacker, Bryan E
et al.

Publication Date

2017-12-01

DOI

10.1016/j.ymthe.2017.08.007

Peer reviewed

Molecular Therapy
Original Article

Guanidinylated Neomycin Conjugation Enhances Intranasal Enzyme Replacement in the Brain

Wenyong Tong,[1] Chrissa A. Dwyer,[1] Bryan E. Thacker,[2] Charles A. Glass,[2] Jillian R. Brown,[2] Kristina Hamill,[3] Kelley W. Moremen,[4] Stéphane Sarrazin,[1] Philip L.S.M. Gordts,[5] Lara E. Dozier,[6] Gentry N. Patrick,[6] Yitzhak Tor,[3] and Jeffrey D. Esko[1]

[1]Department of Cellular and Molecular Medicine, Glycobiology Research and Training Center, University of California, San Diego, La Jolla, CA 92093-0687, USA; [2]TEGA Therapeutics, Inc., 9500 Gilman Drive, La Jolla, CA 92093-0713, USA; [3]Department of Chemistry and Biochemistry, University of California, San Diego, La Jolla, CA 92093-0358, USA; [4]Department of Biochemistry, Complex Carbohydrate Research Center, University of Georgia, Athens, GA 30602, USA; [5]Department of Medicine, University of California, San Diego, La Jolla, CA 92093-0687, USA; [6]Section of Neurobiology, Division of Biological Sciences, University of California, San Diego, La Jolla, CA 92093-0366 USA

Iduronidase (IDUA)-deficient mice accumulate glycosaminoglycans in cells and tissues and exhibit many of the same neuropathological symptoms of patients suffering from Mucopolysaccharidosis I. Intravenous enzyme-replacement therapy for Mucopolysaccharidosis I ameliorates glycosaminoglycan storage and many of the somatic aspects of the disease but fails to treat neurological symptoms due to poor transport across the blood-brain barrier. In this study, we examined the delivery of IDUA conjugated to guanidinoneomycin (GNeo), a molecular transporter. GNeo-IDUA and IDUA injected intravenously resulted in reduced hepatic glycosaminoglycan accumulation but had no effect in the brain due to fast clearance from the circulation. In contrast, intranasally administered GNeo-IDUA entered the brain rapidly. Repetitive intranasal treatment with GNeo-IDUA reduced glycosaminoglycan storage, lysosome size and number, and neurodegenerative astrogliosis in the olfactory bulb and primary somatosensory cortex, whereas IDUA was less effective. The enhanced efficacy of GNeo-IDUA was not the result of increased nose-to-brain delivery or enzyme stability, but rather due to more efficient uptake into neurons and astrocytes. GNeo conjugation also enhanced glycosaminoglycan clearance by intranasally delivered sulfamidase to the brain of sulfamidase-deficient mice, a model of Mucopolysaccharidosis IIIA. These findings suggest the general utility of the guanidinoglycoside-based delivery system for restoring missing lysosomal enzymes in the brain.

INTRODUCTION

All cells produce plasma membrane and extracellular matrix proteoglycans consisting of a protein core with one or more covalently attached glycosaminoglycan (GAG) chains.[1] The proteoglycans undergo endocytosis and delivery to lysosomes, where the GAGs are degraded by a series of lysosomal hydrolases that sequentially process or cleave the non-reducing end (NRE) of the chain. Inactivation of any of the enzymes causes a subgroup of lysosomal storage disorders called mucopolysaccharidoses (MPS). MPS patients accumulate GAGs in the lysosomes of cells in different tissues, causing organomegaly, skeletal abnormalities, heart valve and vascular defects, and early mortality.[2] The accumulation of GAGs in the central nervous system (CNS) causes developmental delay and intellectual disability. As the disease progresses, widespread neurodegeneration and progressive mental retardation occur.[3]

Enzyme-replacement therapy (ERT) involves infusion of patients with recombinant enzyme containing targeting signals to achieve lysosomal delivery.[4] Successful ERT takes advantage of the expression of insulin-like growth factor II/mannose-6-phosphate receptors (IGF-II/M6PR) or C-type mannose receptors on macrophages and the production of recombinant enzymes containing asparagine-linked glycans terminating in mannose-6-phosphate or mannose.[5] Conventional ERT reduces lysosomal storage and disease pathogenesis in peripheral organs but does not reduce disease progression in the brain due to low expression of receptors on blood-brain barrier (BBB) endothelial cells and parenchymal cells in the brain and poor transport across the BBB.[6] Moreover, difficulties can occur in generating recombinant enzymes with appropriate mannose-6-phosphate containing N-glycans. Methods that either facilitate transport of recombinant enzyme across the BBB or bypass the BBB are needed to enable ERT for the CNS.

Nose-to-brain delivery of therapeutics through intranasal administration is a non-invasive approach to bypass the BBB.[7] Wolf and colleagues have reported transport of recombinant α-L-iduronidase (IDUA) (Aldurazyme [Laronidase], IDUA) to the brain of adult mice after intranasal administration, but the pharmacokinetics of enzyme delivery and its impact on storage and neuropathological hallmarks of α-L-IDUA deficiency were not reported.[8] We described a method that enhances delivery of recombinant enzymes to the

Received 25 January 2017; accepted 9 August 2017;
http://dx.doi.org/10.1016/j.ymthe.2017.08.007.

Correspondence: Jeffrey D. Esko, Department of Cellular and Molecular Medicine, University of California, San Diego, La Jolla, CA 92093-0687, USA.
E-mail: jesko@ucsd.edu

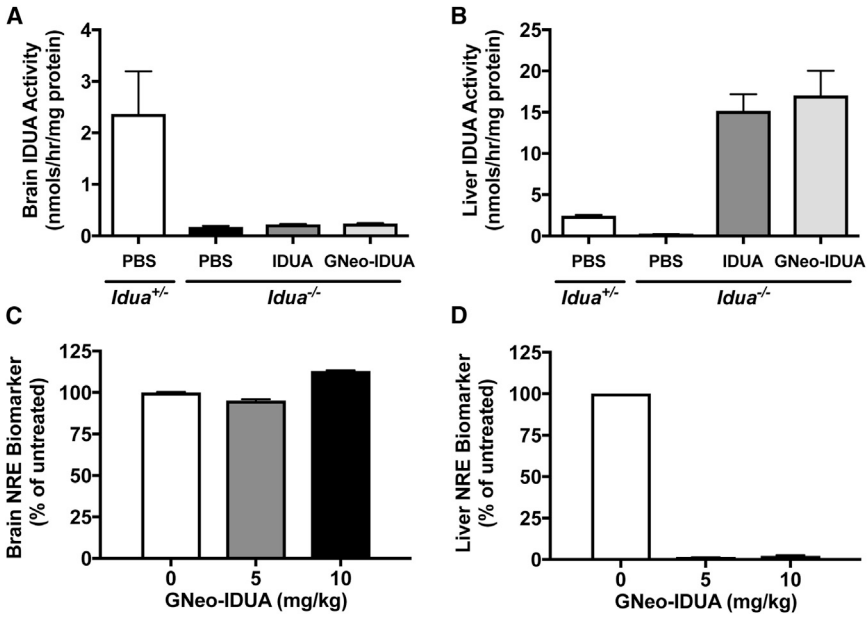

Figure 1. Intravenous Administration of GNeo-Conjugated IDUA Shows Delivery Restricted to Somatic Tissues

MPSI mice (*Idua*$^{-/-}$) were treated intravenously with 5 mg/kg GNeo-IDUA, unconjugated IDUA, or PBS. Tissues were harvested 1 hr following treatment. (A) IDUA enzyme activity in whole brains. (B) IDUA enzyme activity in livers. (C) Non-reducing end heparan sulfate analysis by liquid chromatography/mass spectrometry in whole brains 48 hr after injection of enzyme. (D) Non-reducing end heparan sulfate analysis in livers. n = 2–3 mice per bar. Error bars indicate SEM.

lysosome in cultured cells.[9] The carrier, which consists of a guanidinylated form of neomycin (GNeo), enabled sufficient enzyme delivery to reverse GAG accumulation in human fibroblasts derived from MPS I and MPS VII patients who have germline mutations in α-L-IDUA and β-D-glucuronidase, respectively. The GNeo delivery system harnesses the high-affinity of GNeo for cell-surface heparan sulfate proteoglycans (HSPGs) and their capacity to take up macromolecular cargo by macropinocytosis resulting in delivery to lysosomes.[9–12] In this study, we demonstrate enhanced brain ERT using GNeo-conjugated enzymes and intranasal administration. Sustained intranasal treatment of MPS I mice showed that GNeo-IDUA reduces GAG accumulation and neuropathological hallmarks of disease in the olfactory bulb and cerebral cortex.

RESULTS

Intravenous Injection of GNeo-IDUA Reduces Storage in the Liver, but Not in the Brain

GNeo contains six guanidinium groups in place of the naturally occurring ammonium groups in neomycin (Figure S1A). The arrangement of the fixed, positively charged guanidinium groups complement the negatively charged sulfate and carboxyl groups in heparan sulfate and create the basis of selective, high-affinity interactions with cell-surface HSPGs.[10] In previous studies, we showed that GNeo-conjugated macromolecules bind to and aggregate HSPGs, enter the cells by macropinocytosis, and traffic to lysosomes.[10,11] GNeo-conjugated lysosomal enzymes delivered through this mechanism add to the existing pool of soluble lysosomal enzymes and can reconstitute lysosomal degradation in fibroblasts derived from patients with MPS disorders.[9]

To evaluate the capacity of GNeo to deliver recombinant lysosomal enzymes to the brain, we conjugated the carrier to IDUA and recombinant *N*-sulfoglucosamine sulfohydrolase (sulfamidase [SGSH]), lysosomal enzymes mutated in MPS I and MPS IIIA patients, respectively, and in the corresponding mouse models.[13,14] Initial studies of IDUA utilized Aldurazyme treated with alkaline phosphatase, which reduced by 95% the mannose-6-phosphate content of the preparation. Recombinant SGSH was prepared in HEK cells and had very low amounts of mannose-6-phosphate obviating the need for treatment with alkaline phosphatase (Materials and Methods). GNeo-IDUA and GNeo-SGSH preparations were purified by affinity chromatography on heparin-Sepharose (Figures S1B–S1D). Conjugation of GNeo to enzymes and subsequent chromatography did not alter enzyme-specific activity (Materials and Methods) or enzyme stability toward thermal denaturation (Figure S2A).

To examine if GNeo conjugation facilitated delivery of recombinant enzyme in vivo, we treated MPS I mice deficient in IDUA (*Idua*$^{-/-}$) with GNeo-IDUA by tail-vein injection, and after 1 hr, we collected the brain and liver. IDUA enzyme activity in brain homogenates prepared from IDUA or GNeo-IDUA-treated mice remained at baseline levels, comparable to mice injected with phosphate-buffered saline (PBS) (Figure 1A). In contrast, injection of IDUA or GNeo-IDUA dramatically increased enzyme activity in the liver to levels that exceeded by 7-fold the activity present in heterozygous *Idua*$^{+/-}$ mice (Figure 1B).

The absence of α-L-IDUA in cells and tissues of MPS I mice and patients causes the accumulation of heparan sulfate and chondroitin/dermatan sulfate with iduronic acid residues at the NRE of the chains, which serves as a biomarker of the disease.[15] The NRE biomarker can be detected and quantified following enzymatic digestion of the GAG chains into disaccharides and analysis by liquid chromatography/mass spectrometry.[16] Wild-type and heterozygous carriers express very low levels of glycan biomarkers characteristic of MPS disorders, but tissues and cells derived from mutant mice accumulate very high levels of diagnostic glycan biomarkers. Thus, analysis of NRE biomarkers provides a very sensitive method to assess whether functional enzyme delivery to lysosomes occurs.[16] Analysis of the NRE biomarker characteristic of heparan sulfate storage in MPS I

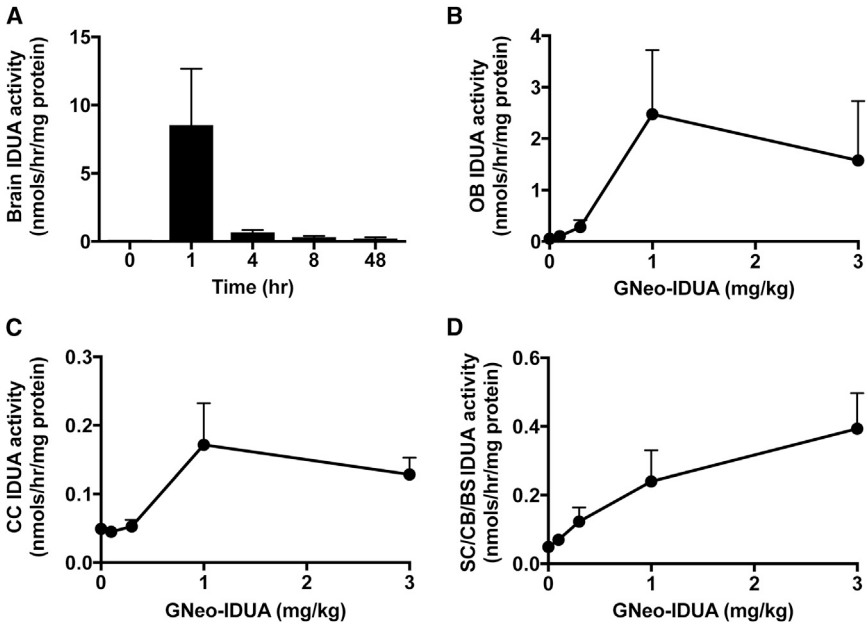

Figure 2. Pharmacokinetic and Biodistribution Analysis of Intranasally Administered GNeo-IDUA in the Brain

(A) *Idua*$^{-/-}$ mice were treated intranasally with 1 mg/kg GNeo-IDUA. IDUA enzyme activity was measured at 0, 1, 4, 8, and 48 hr following treatment. n = 2–4 mice per bar. (B–D) *Idua*$^{-/-}$ mice were treated intranasally with the indicated concentrations of GNeo-IDUA, and different brain regions were collected 1 hr following treatment. n = 3 mice per data point. (B) IDUA enzyme activity in the olfactory bulbs. (C) IDUA enzyme activity in the cerebral cortex (CC). (D) IDUA enzyme activity in subcortical (SC), cerebellum (CB), and brain stem (BS) regions. Error bars indicate SEM.

(iduronate-*N*-sulfoglucosamine [I0S0]) did not reveal any reduction in the brain 48 hr after tail-vein injection of 5 or 10 mg/kg of GNeo-IDUA (Figure 1C). In contrast, the NRE biomarker in the liver was reduced to baseline levels (Figure 1D). These data suggest that GNeo-IDUA did not cross the BBB appreciably but was taken up in the liver where it reduced heparan sulfate accumulation.

Given that BBB endothelial cells, like all animal cells, express abundant HSPGs,[17] the low extent of enzyme uptake into the brain was somewhat surprising. To evaluate the plasma concentration of enzyme, blood samples were taken after injection of GNeo-IDUA. Analysis of enzyme activity indicated fast clearance, with an estimated half-life of ~3 min (Figure S2B). Attempts to improve plasma residence time by adjusting the dose of enzyme from 1–10 mg/kg, by continuous infusion of 3.85 mg/kg for 20 min or 5 mg/kg for 40 min, by repetitive dosing, or by injecting a mixture of enzyme with low molecular weight heparin had no effect on the enzyme half-life in the plasma.

Intranasal Uptake of Enzyme Drives Lysosomal Delivery in the Brain

To find an alternate route to the brain, we examined intranasal delivery of IDUA, which Wolf and colleagues showed to result in small amounts of enzyme distributed throughout the brain.[8] This delivery route bypasses the BBB as a result of direct nose-to-brain diffusion along perineural/perivascular routes or by transport through olfactory sensory neurons.[18,19] Intranasal administration of IDUA and GNeo-IDUA led to striking uptake of enzyme into the brains of *Idua*$^{-/-}$ mice within 1 hr, reaching levels comparable to the amount of enzyme present in heterozygous mice (Figure S3A). Similar results were obtained in a study of GNeo-SGSH and unconjugated SGSH (Figure S3B).

A basic pharmacokinetic study of GNeo-IDUA in the brain showed that the amount of enzyme activity peaked 1 hr post-administration and decreased over the next 4 hr (Figure 2A). A small but significant amount of enzyme was retained even at 48 hr. Similar pharmacokinetic behavior was observed after intranasal administration of GNeo-SGSH to mice (Figure S4). GNeo-IDUA distributed throughout all brain regions, including the olfactory bulbs (Figure 2B), the cerebral cortex (Figure 2C), subcortical regions, cerebellum, and the brain stem (Figure 2D), with the highest levels in the olfactory bulbs. Transport into the brain appeared to be saturable with respect to concentration in the olfactory bulb and cerebral cortex, reaching a maximum at ~1 mg/kg (Figures 2B–2D). Uptake of enzyme into the brain occurred most likely by a direct route as opposed to retrograde transport, based on the rapid appearance of enzyme throughout the brain. It seems unlikely that enzyme entering the circulation through the olfactory vascular beds was a source, given the rapid clearance rate from the plasma (Figure S2B). Attempts to localize the enzyme by immunohistochemistry were unsuccessful using several different antibody preparations.

GNeo-IDUA Enhances the Reduction of GAG in the Brain

The rapid turnover of enzyme from the brain suggested that most of it was initially in the extracellular space and not taken up by cells. To determine if the delivery of IDUA to the brain resulted in delivery to lysosomes and reduction of GAGs, we administered IDUA and GNeo-IDUA intranasally to *Idua*$^{-/-}$ mice every other day (e.o.d.) for 14, 30, and 60 days. Reduction of the NRE biomarker occurred with both enzyme preparations, but GNeo-IDUA was more effective (Figure 3A). Treatment with GNeo-IDUA also significantly reduced total GAG (heparan sulfate and chondroitin sulfate) as measured by carbazole reaction, whereas treatment with IDUA was less effective (Figures S5A–S5C). Increasing the frequency of GNeo-IDUA treatment to twice a day (b.i.d.) for 14 days significantly reduced NRE levels compared to mice treated with unconjugated IDUA (Figure 3B). A parallel study in which *Sgsh*$^{-/-}$ mice were dosed intranasally with GNeo-SGSH (1 mg/kg) for 30 days e.o.d. also showed enhanced reduction of the MPS IIIA NRE biomarker (*N*-sulfoglucosamine) when compared to SGSH treatment (Figure S6).

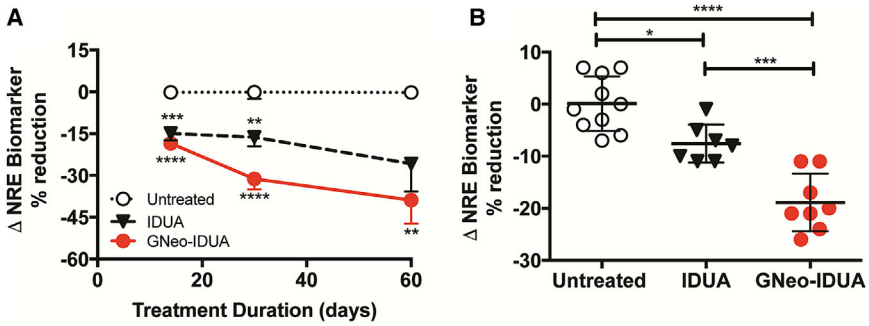

Figure 3. GNeo-IDUA Reduces the NRE Heparan Sulfate Biomarker in the MPSI Mouse Brain

(A) *Idua*$^{-/-}$ mice were treated intranasally with 1 mg/kg IDUA or GNeo-IDUA every other day for 14, 30, and 60 days. n = 10–12 mice for 14 days and 30 days; n = 5–6 mice for 60 days. (B) *Idua*$^{-/-}$ mice were treated intranasally with 1 mg/kg IDUA or GNeo-IDUA twice a day for 14 days. n = 7–10 mice per treatment group from two separate experiments. Non-reducing end biomarker was determined in heparan sulfate isolated from whole brains. *p < 0.05, **p < 0.01, ***p < 0.001, ****p < 0.0001. Error bars indicate SEM, and significance was determined by one-way analysis of variance (ANOVA) with Tukey's post-hoc analysis.

GNeo-IDUA Ameliorates Lysosome Expansion and Astrogliosis in Aged MPSI Mice

Lysosomal accumulation of GAG in MPS disorders causes expansion of the lysosomal compartment in all cell types in the brain and reactive astrogliosis, a histological hallmark of neurodegeneration.[14] To determine if the more dramatic reduction of GAG and NRE biomarker observed after intranasal treatment with GNeo-IDUA correlated with reduced neuropathology, we treated *Idua*$^{-/-}$ mice intranasally with 1 mg/kg IDUA or GNeo-IDUA. The treatment protocol initiated with intranasal administration b.i.d. for 30 days followed by treatment once daily for 30 days. As expected brains from untreated *Idua*$^{-/-}$ mice stained strongly for LAMP1, a lysosomal membrane marker, and glial fibrillary protein (GFAP), a marker of astrogliosis (Figure 4). Intranasal treatment with IDUA had little if any effect on LAMP1 accumulation and astrogliosis in the olfactory bulb and primary somatosensory cortex (Figure 4). In contrast, treatment with GNeo-IDUA normalized LAMP1 and GFAP immunoreactivity in the olfactory bulb (Figures 4A–4C), with significant reductions noted in the primary somatosensory cortex, which is caudal to the olfactory bulb (Figures 4D–4F). Thin section electron micrographs of the cerebral cortex showed that GNeo-IDUA also reduced the quantity of lysosomal storage vesicles in neuronal cells, whereas IDUA did not (Figure 5).

As noted in Figure S3, the level of GNeo-IDUA and IDUA uptake into the brain did not differ significantly in short-term experiments. To explain the enhanced ability of GNeo-conjugated enzyme to reduce the NRE biomarkers and neuropathological markers, we incubated cultures of primary rat cortical neurons and astrocytes with GNeo-IDUA and IDUA, trypsin treated the cells to remove surface-bound enzyme, and then measured enzyme activity. GNeo-IDUA was internalized more efficiently than IDUA in mixed cortical neuron and astrocyte culture, indicating that the enhanced reduction of GAG, NRE biomarker, and neuropathological markers most likely arose from enhanced enzyme uptake in neural cells, as observed previously in cultured fibroblasts (Figure 6).[9]

DISCUSSION

Conventional ERT depends on both mannose-6-phosphate recognition markers on the therapeutic enzyme and expression of IGF-II/M6PR on recipient cells. However, difficulties can arise in the production of recombinant enzyme with asparagine-linked glycans suitably modified with mannose-6-phosphate residues,[20–22] and the level of IGF-II/M6PR on cells varies. The expression of IGF-II/M6PR on BBB endothelial cells declines progressively in mice from levels adequate to facilitate enzyme delivery across the BBB in neonates to a total lack of expression in adult mice.[23] Overall, the brain contains lower levels of IGF-II/M6PR compared to other organs,[24] which may partially contribute to the difficulty in achieving fully restorative ERT in the CNS. One way to enhance lysosomal enzyme transport across the BBB is through pharmacologic manipulation of mannose-6-phosphate receptors.[25] Another approach involves oxidation of the glycans with periodate, which improves plasma half-life and uptake into the brain.[26] Other receptors can be exploited, for example C-type mannose receptors, but their expression is limited to macrophages and a few other cell types.[27] Recent efforts have focused on the development of chimeras of lysosomal enzymes fused to peptides or antibodies that recognize ubiquitously distributed receptors for transferrin, insulin, or lipoproteins.[28–30] Unfortunately, this approach has met with limited success due to inefficient delivery to the parenchyma of the brain or unanticipated side effects (reviewed by Sands).[31]

Other methods to introduce recombinant lysosomal enzymes into the brain are currently under development. These include direct injection of recombinant enzymes into the cerebral spinal fluid (CSF) through intraventricular or intrathecal administration.[32,33] Kan and colleagues showed effective delivery of a fusion protein of recombinant α-*N*-acetylglucosaminidase and a fragment of IGF-II administered intracerebroventricularly to the brain of adult MPSIIIB mice.[34,35] Cell-based enzyme replacement therapies, which introduce cells that secrete enzyme into the brain, have also been accomplished by allogeneic hematopoietic stem cell transplantation (HSCT). Both of these methods have associated risks, as infusion of enzyme directly into the brain requires installation of access ports into the skull, and HSCT has a limited success rate in MPS patients.[36–38] Adenoviral gene therapy has great promise, but long-term effects of gene therapy are unknown.[39,40]

We were inspired to examine the possibility of exploiting HSPGs as a portal of entry into the cell based on studies of lipoprotein uptake in hepatocytes, which depends on apolipoprotein binding to the

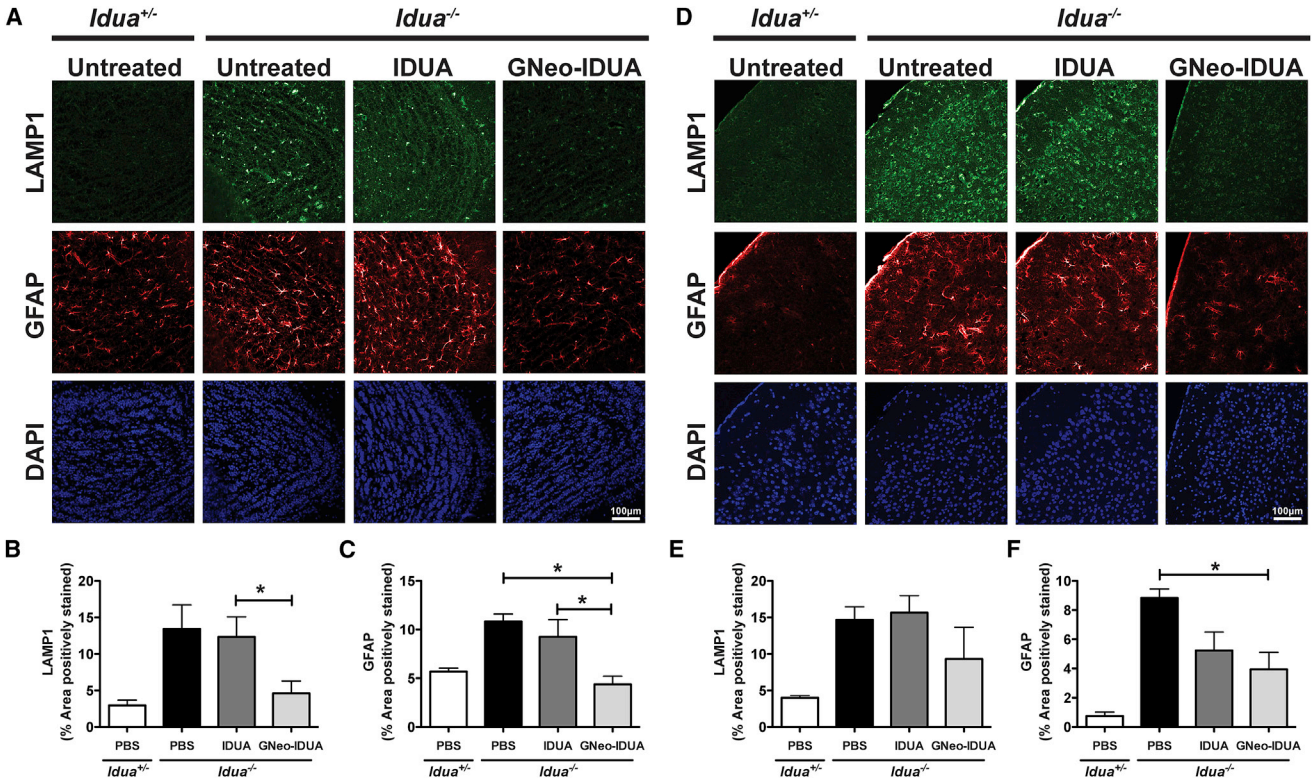

Figure 4. GNeo-IDUA Reduces Histopathological Hallmarks in the Aged MPSI Mouse Brain

Idua$^{-/-}$ mice were treated intranasally with 1 mg/kg IDUA or GNeo-IDUA twice a day for 30 days and then once a day for 30 days. Coronal sections were taken from different brain regions and stained with antibodies against LAMP1, a lysosomal marker, or GFAP, a marker of astrocytosis. (A) Representative confocal images acquired from olfactory bulbs. (B) Quantification of LAMP1 and (C) GFAP in the granule cell layer of the olfactory bulb. (D) Representative confocal images acquired from the primary somatosensory cortex. (E) Quantification of LAMP1 and (F) GFAP in layer II/III of the primary somatosensory cortex. n = 3 animals per treatment group. Error bars indicate SEM, and significance was determined by one-way analysis of variance (ANOVA) with Tukey's post-hoc analysis.

heparan sulfate chains of the proteoglycan syndecan-1.[41] Moreover, all cells express HSPGs, and studies have shown that endocytosis of HSPGs occurs constitutively in most cells.[42] Indeed, it is the uptake, lysosomal delivery, and subsequent degradation of HSPGs that goes awry in MPS syndromes. We have described molecular transporters based on polycationic glycosides such as GNeo and other naturally occurring aminoglycosides.[10,12] The per-guanidinylated derivatives bind with high selectivity and affinity to heparan sulfate, thus suggesting their potential use as molecular carriers for lysosomal enzyme replacement. Sarrazin et al. showed that conjugation of GNeo to α-L-IDUA and β-D-glucuronidase reconstitutes enzyme activity and completely resolves GAG storage in fibroblasts from MPSI and MPS VII patients, respectively.[9] Comparisons made to unconjugated enzyme clearly demonstrated enhanced enzyme uptake and GAG resolution with the GNeo carrier.[9] The findings reported here demonstrate that GNeo-conjugated IDUA is capable of restoring lysosomal degradation of GAGs in the liver and brain, consistent with the widespread expression of HSPGs by hepatocytes, neurons, glial cells, and other cell types.[43] Enhanced delivery of adenoviral delivered β-D-glucuronidase engineered with the TAT peptide also occurs through HSPG-dependent uptake mechanisms,[44,45] documenting the utility of HSPGs as endocytic receptors for therapeutic delivery.

Numerous studies have shown that biologics administered intranasally enter the brain through one or more possible routes, including diffusion along perivascular paths, transport via olfactory and trigeminal nerves, direct uptake and transport by olfactory sensory neurons, or by lymphatic perfusion.[46] Our findings do not suggest that GNeo conjugation enhances nose-to-brain delivery per se or through any particular route but rather enhances either retention of enzyme in the parenchyma of the brain and/or lysosomal delivery in cells. The level of delivery of enzymes varied in different experiments, which may depend in part on the method used to assess enzyme levels, the cargo, and the age of the animals. Nevertheless, in short-term experiments, the level of delivered enzyme was comparable to that found in the brain of heterozygous animals. Our findings show that enzyme introduced in this way clears rapidly from the brain, but a small amount is retained. Apparently, sufficient enzyme accumulates over time to reduce storage and neuropathological markers. Complete restoration of NRE biomarker levels and neuropathological markers was not obtained in the time frame of these experiments, but the

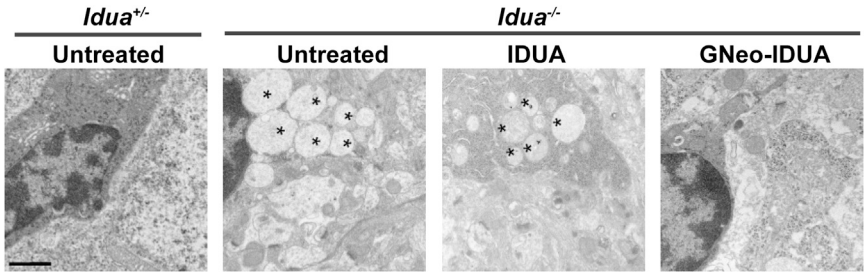

Figure 5. GNeo-IDUA Reduces Lysosomal Storage in the MPSI Cerebral Cortex

Electron microscopy images show that the number of lysosomal storage vesicles (asterisks) is reduced following GNeo-IDUA treatment. Scale bar, 1 μm.

results encourage additional studies in which the dose and duration of treatment are varied. Long term intranasal treatment coupled with intravenous therapy is needed to assess the impact on behavior and survival.

A key finding presented here is that introduction of GNeo-conjugated IDUA led to greater reductions of accumulated heparan sulfate NRE biomarkers, total GAG, lysosomes, and activated astrocytes in MPSI mice compared to unconjugated enzyme. These findings show GNeo conjugation enhances the efficacy of intranasal ERT to the brain. Enhanced efficacy might be obtained by modifying technical aspects of the delivery system. The method of delivery by instillation of enzyme droplets into the nose is primitive and could be vastly improved with enhanced delivery devices that target the olfactory epithelium and/or by inclusion of mucoadhesive adjuvants.[47] We recently reported that liposomes containing GNeo-conjugated lipids (GNeosomes) also traffic to lysosomes by way of HSPG-mediated endocytosis.[48,49] This finding raises the possibility of packaging unconjugated enzymes in GNeosomes, which might improve delivery intranasally or intravenously.

The observation that other types of neurodegenerative disorders can be accompanied by lysosomal dysfunction suggests that GNeo might prove useful to enhance lysosomal enzyme or protein delivery therapies for other diseases that affect the brain.[50] By modulating the structure of the guanidinylated glycoside or the linker between the glycoside and the cargo, one might be able to design transporters with other desirable attributes, such as reversibility and release from the endosome-lysosomal pathway for delivery to the cytoplasm, nucleus, or other organelles.

MATERIALS AND METHODS

Recombinant Enzymes

Human recombinant α-L-IDUA (Aldurazyme; Laronidase) was provided by Genzyme (Cambridge, MA) and processed by heparin-Sepharose chromatography to remove excipients. In the experiments shown in Figures 1, 2, and 3, IDUA was treated with alkaline phosphatase, which reduced the molar ratio of mannose-6-phosphate/enzyme from 20 to 3. Initial studies showed that removal of the mannose-6-phosphate targeting signal had no effect on enzyme uptake, and therefore in subsequent experiments excipient free enzyme was conjugated to GNeo.

Recombinant SGSH was produced by expression of His_6-tagged or Myc-His_6 tagged murine SGSH in HEK293 cells. An expression plasmid containing the coding sequence for SGSH (pXLG-SGSH) was spliced into pcDNA3 vectors (Invitrogen, Carlsbad, CA) containing a C-terminal His_6- or Myc-His_6-tag. FreeStyle 293F cells (Thermo Fisher Scientific, Waltham, MA) were transfected with the expression plasmids (3 μg/ml DNA, 9 μg/ml PEI) and selected by addition of 600 μg/ml G418. A single cell colony was selected for maximum enzyme production. Enzyme was produced by culturing the cells in 1 l shaker flasks containing 300 ml of FreeStyle 293 Expression Medium (Thermo Fisher Scientific) for 6 days. Cells were removed by centrifugation, and the enzyme was purified from the conditioned medium using a Ni^{2+} column as previously described.[51] Analysis of the *N*-linked oligosaccharides revealed the presence of <0.2 mole mannose-6-phosphate residues/mole of enzyme in the SGSH preparation. The various IDUA preparations had enzyme-specific activities of 5–6 U/mg using 4-methylumbelliferyl α-L-iduronide as substrate (Affymetrix, Santa Clara, CA), whereas SGSH preparations had activities that ranged from 70 to 150 mU/mg using 4-MU-α-D-N-sulfoglucosaminide (Moscerdam, the Netherlands/Carbosynth, San Diego, CA) as substrate.

GNeo-NHS Synthesis and Enzyme Conjugation

GNeo-NHS was synthesized as described previously.[48] Conjugation reactions for IDUA and SGSH were preformed at 4°C by incubating GNeo-NHS and enzyme at ratios ranging from 50:1 to 125:1 (mol/mol) in order to achieve a comparable level of binding to heparin-Sepharose (Hi-Trap Heparin-HP 1 ml; GE Biosciences, Pittsburgh, PA). GNeo-conjugated enzymes were eluted from the column using a continuous 0.15 M to 2 M NaCl gradient in phosphate buffer (pH 7.4) by fast-protein liquid chromatography and monitoring elution by absorbance at 280 nm (see Figures S1B–S1D). Fractions containing GNeo-conjugated enzyme were combined, de-salted, and concentrated using 10-kDa molecular mass cutoff filters (Amicon Ultra; Millipore, Temecula CA). The final concentration of enzyme was determined by Pierce bichinchoninic acid assay (BCA) protein assay kit (Thermo Fisher Scientific).

Mice

An MPSI mouse model carrying an engineered germline-null allele for *Idua* (B6.129-*Iduatm1Clk*/J, referred to as $Idua^{-/-}$)[14] and an MPSIIIA mouse model carrying a spontaneous missense mutation resulting in a hypomorphic allele for *Sgsh* (B6.Cg-Sgshmps3a/PstJ, referred to as $Sgsh^{h/h}$)[13] were purchased from Jackson Laboratory (Bar Harbor, ME). Animals carrying an engineered germline-null allele of $Sgsh^{-/-}$ were generated as described.[3] All mice were backcrossed for ≥10

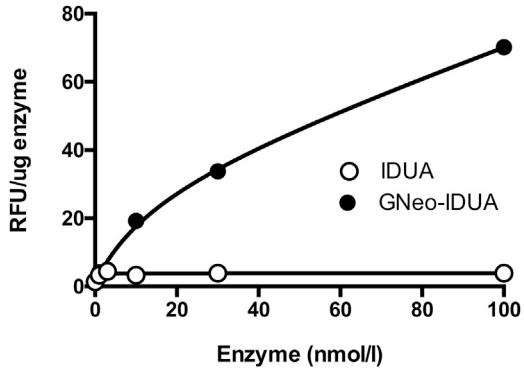

Figure 6. Enhanced Uptake of GNeo-IDUA in Rat Neurons

Cultures of primary rat cortical neurons and astrocytes were treated with the indicated concentration of IDUA or GNeo-IDUA for 2 hr. The cells were washed, trypsin treated, sedimented by centrifugation, washed twice, and subsequently assayed for iduronidase activity. Each data point represents a single well. The experiment was performed twice with comparable findings.

generations onto a C57BL/6 background. Animals were housed and bred in vivaria approved by the Association for Assessment and Accreditation of Laboratory Animal Care located in the School of Medicine, UCSD, following standards and procedures approved by the UCSD Institutional Animal Care and Use Committee.

Dosing

All mice were 12–13 weeks of age, unless otherwise specified. In some experiments, animals were immobilized and injected via the tail vein with $\leq$ 0.1 ml of enzyme solution in PBS to achieve the indicated dosage. Sublingual blood samples were collected for enzyme activity measurements. For intranasal administration, mice were lightly anesthetized using isoflurane (Fluriso; VetOne, Boise, ID) delivered using a SurgiVetH Vaporstick (Dublin, OH) small animal anesthesia machine equipped with a Classic T3TM isoflurane vaporizer. Mice were exposed to 3% isoflurane delivered in oxygen (1 l/min) within a 1 l induction chamber until a state of areflexia was reached. The mice were turned to a supine position, and a micropipette was used to administer 3 μl aliquots of enzyme in the left and right nares until the final dose was administered (usually 1 mg/kg). After each instillation, the mice were returned to the isoflurane chamber in a prone position.

To harvest tissues and blood, mice were heavily anesthetized using isoflurane or a mixture of ketamine/xylazine and perfused transcardially with Dulbecco's PBS (dPBS). Organs were harvested and homogenized with a Polytron (Montreal, Canada) homogenizer in 2–3 volumes (w/v) of PBS containing 0.1% Triton X-100. Samples were centrifuged at 10,000 × *g*, and supernates were used for assay of IDUA and SGSH.

Uptake of Enzyme by Rat Neurons

Rat dissociated cortical neurons and astrocytes from post-natal day 1 animals of either sex were plated onto poly-D-lysine coated 6-well plates at a density of 500,000 cells per well. The cells were cultured to maturation for 14–21 days in vitro (DIV) in B27 supplemented Neurobasal Medium (Invitrogen) as previously described.[52] Enzymes were added to the wells at the concentrations indicated in the figure legends. The cells were incubated for 2 hr at 37°C, washed twice with PBS, treated with trypsin/EDTA, and then combined with complete medium to inhibit the trypsin. Cells were sedimented by centrifugation and resuspended in 200 μL of lysis buffer (PBS, 0.5% TX-100 and a mixture of protease inhibitors [Roche]). Enzyme activity in the cell extracts was measured as described below.

Enzyme Assays

IDUA activity was measured by assaying the conversion of 4-methylumbelliferyl α-L-Iduronide (4-MU Iduronide; Glycosyn) into the fluorochrome 4-methylumbelliferone (4-MU). The assay was performed in 50 μl of 200 mM sodium formate (pH 3.5) buffer containing 50 μM 4-MU Iduronide substrate and varying amounts of enzyme, cell or tissue extract. After 30 min at 37°C, fluorescent 4-MU product was measured by fluorimetry (excitation 360 nm, emission 460 nm). Enzyme activity was normalized to protein concentration measured by BCA assay. Enzyme mass was determined using a standard curve generated with recombinant enzyme. For SGSH enzyme activity assays, recombinant SGSH carrying a His_6-tag was captured from tissue homogenates using Ni^{2+} beads prior to performing enzyme activity assays. Activity was measured using 4-methylumbelliferyl *N*-sulfo-β-D-glucosamine as described.[13]

SGSH ELISA Assay

An anti-His tag antibody (GenScript, Piscataway, NJ) was immobilized on 96-well microtiter plates. Wells were blocked with 1% BSA diluted in phosphate buffered saline with Tween-20 (PBST) for 1 hr. Brain homogenate from treated animals was added to wells and incubated for 1 hr at room temperature. Recombinant Myc-His_6-SGSH was detected using a polyclonal anti-Myc antibody (Abcam, Cambridge, UK) followed by an anti-rabbit secondary antibody conjugated to horseradish peroxidase (HRP; Jackson Immunoresearch, West Grove, PA) and TMB Turbo ELISA substrate (Thermo Fisher Scientific). The amount of recombinant Myc-His_6-SGSH was quantified using a standard curve of Myc-His_6-SGSH spiked into a mouse brain homogenate.

Glycosaminoglycan Purification and Analysis

After whole-animal perfusion, livers and whole brains were removed and dissected as indicated. Tissues were homogenized in ice-cold buffer containing 50 mM sodium acetate (pH 6.0) and 0.2 M sodium chloride using a Polytron homogenizer. GAGs were purified as described previously.[53] NRE analysis of purified heparan sulfate was determined.[16] The NRE glycan biomarkers for MPSI and MPSIIIA are I0S0 and *N*-sulfoglucosamine, respectively.[16] In some experiments, total GAGs were quantitated by measurement of uronic acid.[54]

Immunohistochemistry

Mice were heavily anesthetized using a mixture of ketamine/xylazine and transcardially perfused with dPBS followed by 4% phosphate-buffered paraformaldehyde (PB-PFA). Whole brains were dissected

and post-fixed in 4% PB-PFA overnight at 4°C. Brains were cryoprotected by sinking in 30% sucrose in 0.1 M phosphate buffer and embedded in O.C.T. compound (Tissue-Tek, Torrance, CA) in a bath of dry ice and isopentane. Coronal sections (12 μ) were prepared using a cryostat and mounted directly onto glass slides and fixed with 4% PB-PFA for 5 min. Sections were blocked and stained in 3% bovine serum albumin, 0.5% Triton X-100 diluted in PBS with 0.05% Tween 20. Sequential staining was performed using a monoclonal antibody for LAMP1 (clone 1D4B, developed by Thomas August, was obtained from the Developmental Studies Hybridoma Bank at The University of Iowa) followed by GFAP (clone G-A-5; Sigma-Aldrich, St. Louis, MO). Nuclei were stained with DAPI. Confocal images were collected on a Nikon Ti microscope (Tokyo, Japan) equipped with the Nikon A1R confocal systems using a 10× or 20× objective. The ND acquisition tool was used to acquire z stacks in three channels in the Nikon Elements software package. An experimenter blinded to treatment group performed image acquisition and quantification. Data quantification is from two regions of interest within the specified brain region per image. Two or three images were acquired in two different sections that spanned a distance of 120 μ per brain. The percent area positively stained for LAMP1 or GFAP was quantified in the granule layer of the main olfactory bulb or layer II/III of the primary somatosensory cortex using ImageJ software. Percent area calculations for each mouse were averaged and used for statistical analysis.

Electron Microscopy

Blocks (1 mm) of the cerebral cortex were fixed by immersion in modified Karnovsky's fixative (2.5% glutaraldehyde and 2% paraformaldehyde in 0.15 M sodium cacodylate buffer [pH 7.4]) for at least 4 hr. Tissue blocks were post-fixed in 1% osmium tetroxide in 0.15 M cacodylate buffer for 1 hr and incubated en bloc in 2% uranyl acetate for 1 hr to enhance contrast. Samples were dehydrated in ethanol, embedded in Durcupan epoxy resin (Sigma-Aldrich), sectioned at 50 to 60 nm on a Leica UCT ultra-microtome, and picked up on Formvar and carbon-coated copper grids. Sections were stained with 2% uranyl acetate for 5 min and Sato's lead stain for 1 min. Grids were viewed using a JEOL 1200EX II (JEOL, Peabody, MA) transmission electron microscope and photographed using a digital camera (Gatan, Pleasanton, CA) or viewed using a Tecnai G^2 Spirit BioTWIN transmission electron microscope equipped with an Eagle 4k HS digital camera (FEI, Hillsboro, OR). Sections were analyzed at 6400 magnification.

Statistical Analysis

One-way ANOVA with Tukey's post-hoc analysis for comparison was applied for data analysis (*$p < 0.05$, **$p < 0.01$, ***$p < 0.001$).

SUPPLEMENTAL INFORMATION

Supplemental Information includes six figures and can be found with this article online at http://dx.doi.org/10.1016/j.ymthe.2017.08.007.

AUTHOR CONTRIBUTIONS

W.T., C.A.D., B.E.T., C.A.G., K.H., and J.R.B. performed experiments; W.T., C.A.D., B.E.T., C.A.G., P.L.S.M.G., and J.D.E. wrote the manuscript; K.W.M., L.E.D., and G.N.P. provided reagents; S.S. and P.L.S.M.G. provided helpful suggestions; Y.T. and J.D.E. provided support.

CONFLICTS OF INTEREST

W.T., Y.T., and J.D.E. declare pending patents related to the technology disclosed in the paper. C.A.G., B.E.T., J.R.B., Y.T., J.D.E., and the University of California, San Diego have a financial interest in TEGA Therapeutics, which has licensed technology contained in this manuscript. These parties may financially benefit from this interest if the company is successful in marketing its products that are related to this research. The terms of this arrangement have been reviewed and approved by the University of California, San Diego in accordance with its conflict of interest policies.

ACKNOWLEDGMENTS

The project was supported by an NIH Lysosomal Disease Network post-doctoral fellowship (to W.T.) and grants from the MPS Society, the Improved Therapies for MPS I Program through the University of Pennsylvania, the CURE Sanfilippo foundation (to J.D.E.), NIH T32 HL086344 fellowship (to C.A.D.), and grant R43 NS089383 (to C.A.G.). Y.T. thanks the George W. and Carol A. Lattimer endowment for generous support. Genzyme kindly provided Aldurazyme. We thank Chelsea Nora and Gloria Lee for genotyping, as well as the UCSD Electron Microscopy Facility, the UCSD Shared Microscope Facility, the UCSD GRTC GlycoAnalytics Core, the NIH Cancer Center Specialized Support Grant P30 CA23100, and support from NIH grant P41 GM103390 at the University of Georgia.

REFERENCES

1. Esko, J.D., and Selleck, S.B. (2002). Order out of chaos: assembly of ligand binding sites in heparan sulfate. Annu. Rev. Biochem. *71*, 435–471.
2. Neufeld, E.F., and Muenzer, J. (2001). The mucopolysaccharidoses. In Metabolic and Molecular Basis of Inherited Disease, Eighth Edition, *Volume 3*, C.R. Scriver, W.S. Sly, B. Childs, A.L. Beaudet, D. Valle, K.W. Kinzler, and B. Vogelstein, eds. (MacGraw-Hill), pp. 3421–3452.
3. Dwyer, C.A., Scudder, S.L., Lin, Y., Dozier, L.E., Phan, D., Allen, N.J., Patrick, G.N., and Esko, J.D. (2017). Neurodevelopmental changes in excitatory synaptic structure and function in the cerebral cortex of Sanfilippo syndrome IIIA mice. Sci. Rep. *7*, 46576.
4. Kelly, J.M., Bradbury, A., Martin, D.R., and Byrne, M.E. (2017). Emerging therapies for neuropathic lysosomal storage disorders. Prog. Neurobiol. *152*, 166–180.
5. Oh, D.B. (2015). Glyco-engineering strategies for the development of therapeutic enzymes with improved efficacy for the treatment of lysosomal storage diseases. BMB Rep. *48*, 438–444.
6. Lachmann, R.H. (2011). Enzyme replacement therapy for lysosomal storage diseases. Curr. Opin. Pediatr. *23*, 588–593.
7. Lochhead, J.J., and Thorne, R.G. (2012). Intranasal delivery of biologics to the central nervous system. Adv. Drug Deliv. Rev. *64*, 614–628.
8. Wolf, D.A., Hanson, L.R., Aronovich, E.L., Nan, Z., Low, W.C., Frey, W.H., 2nd, and McIvor, R.S. (2012). Lysosomal enzyme can bypass the blood-brain barrier and reach the CNS following intranasal administration. Mol. Genet. Metab. *106*, 131–134.
9. Sarrazin, S., Wilson, B., Sly, W.S., Tor, Y., and Esko, J.D. (2010). Guanidinylated neomycin mediates heparan sulfate-dependent transport of active enzymes to lysosomes. Mol. Ther. *18*, 1268–1274.
10. Elson-Schwab, L., Garner, O.B., Schuksz, M., Crawford, B.E., Esko, J.D., and Tor, Y. (2007). Guanidinylated neomycin delivers large, bioactive cargo into cells through a heparan sulfate-dependent pathway. J. Biol. Chem. *282*, 13585–13591.

11. Inoue, M., Tong, W., Esko, J.D., and Tor, Y. (2013). Aggregation-mediated macromolecular uptake by a molecular transporter. ACS Chem. Biol. *8*, 1383–1388.
12. Dix, A.V., Fischer, L., Sarrazin, S., Redgate, C.P., Esko, J.D., and Tor, Y. (2010). Cooperative, heparan sulfate-dependent cellular uptake of dimeric guanidinoglycosides. ChemBioChem *11*, 2302–2310.
13. Bhaumik, M., Muller, V.J., Rozaklis, T., Johnson, L., Dobrenis, K., Bhattacharyya, R., Wurzelmann, S., Finamore, P., Hopwood, J.J., Walkley, S.U., and Stanley, P. (1999). A mouse model for mucopolysaccharidosis type III A (Sanfilippo syndrome). Glycobiology *9*, 1389–1396.
14. Clarke, L.A., Russell, C.S., Pownall, S., Warrington, C.L., Borowski, A., Dimmick, J.E., Toone, J., and Jirik, F.R. (1997). Murine mucopolysaccharidosis type I: targeted disruption of the murine alpha-L-iduronidase gene. Hum. Mol. Genet. *6*, 503–511.
15. Lawrence, R., Brown, J.R., Lorey, F., Dickson, P.I., Crawford, B.E., and Esko, J.D. (2014). Glycan-based biomarkers for mucopolysaccharidoses. Mol. Genet. Metab. *111*, 73–83.
16. Lawrence, R., Brown, J.R., Al-Mafraji, K., Lamanna, W.C., Beitel, J.R., Boons, G.J., Esko, J.D., and Crawford, B.E. (2012). Disease-specific non-reducing end carbohydrate biomarkers for mucopolysaccharidoses. Nat. Chem. Biol. *8*, 197–204.
17. Wang, L., Fuster, M., Sriramarao, P., and Esko, J.D. (2005). Endothelial heparan sulfate deficiency impairs L-selectin- and chemokine-mediated neutrophil trafficking during inflammatory responses. Nat. Immunol. *6*, 902–910.
18. Thorne, R.G., Pronk, G.J., Padmanabhan, V., and Frey, W.H., 2nd (2004). Delivery of insulin-like growth factor-I to the rat brain and spinal cord along olfactory and trigeminal pathways following intranasal administration. Neuroscience *127*, 481–496.
19. Mustafa, G., Alrohaimi, A.H., Bhatnagar, A., Baboota, S., Ali, J., and Ahuja, A. (2016). Brain targeting by intranasal drug delivery (INDD): a combined effect of trans-neural and para-neuronal pathway. Drug Deliv. *23*, 933–939.
20. Zhao, K.W., and Neufeld, E.F. (2000). Purification and characterization of recombinant human alpha-N-acetylglucosaminidase secreted by Chinese hamster ovary cells. Protein Expr. Purif. *19*, 202–211.
21. Weber, B., Hopwood, J.J., and Yogalingam, G. (2001). Expression and characterization of human recombinant and alpha-N-acetylglucosaminidase. Protein Expr. Purif. *21*, 251–259.
22. Liu, L., Lee, W.S., Doray, B., and Kornfeld, S. (2017). Engineering of GlcNAc-1-phosphotransferase for production of highly phosphorylated lysosomal enzymes for enzyme replacement therapy. Mol. Ther. Methods Clin. Dev. *5*, 59–65.
23. Urayama, A., Grubb, J.H., Sly, W.S., and Banks, W.A. (2008). Mannose 6-phosphate receptor-mediated transport of sulfamidase across the blood-brain barrier in the newborn mouse. Mol. Ther. *16*, 1261–1266.
24. Nissley, P., Kiess, W., and Sklar, M. (1993). Developmental expression of the IGF-II/mannose 6-phosphate receptor. Mol. Reprod. Dev. *35*, 408–413.
25. Urayama, A., Grubb, J.H., Sly, W.S., and Banks, W.A. (2016). Pharmacologic manipulation of lysosomal enzyme transport across the blood-brain barrier. J. Cereb. Blood Flow Metab. *36*, 476–486.
26. Huynh, H.T., Grubb, J.H., Vogler, C., and Sly, W.S. (2012). Biochemical evidence for superior correction of neuronal storage by chemically modified enzyme in murine mucopolysaccharidosis VII. Proc. Natl. Acad. Sci. USA *109*, 17022–17027.
27. Allavena, P., Chieppa, M., Monti, P., and Piemonti, L. (2004). From pattern recognition receptor to regulator of homeostasis: the double-faced macrophage mannose receptor. Crit. Rev. Immunol. *24*, 179–192.
28. Osborn, M.J., McElmurry, R.T., Peacock, B., Tolar, J., and Blazar, B.R. (2008). Targeting of the CNS in MPS-IH using a nonviral transferrin-alpha-L-iduronidase fusion gene product. Mol. Ther. *16*, 1459–1466.
29. Meng, Y., Sohar, I., Sleat, D.E., Richardson, J.R., Reuhl, K.R., Jenkins, R.B., Sarkar, G., and Lobel, P. (2014). Effective intravenous therapy for neurodegenerative disease with a therapeutic enzyme and a peptide that mediates delivery to the brain. Mol. Ther. *22*, 547–553.
30. Boado, R.J., Hui, E.K., Lu, J.Z., Zhou, Q.H., and Pardridge, W.M. (2011). Reversal of lysosomal storage in brain of adult MPS-I mice with intravenous Trojan horse-iduronidase fusion protein. Mol. Pharm. *8*, 1342–1350.
31. Sands, M.S. (2014). A Hitchhiker's guide to the blood-brain barrier: in trans delivery of a therapeutic enzyme. Mol. Ther. *22*, 483–484.
32. Dickson, P., McEntee, M., Vogler, C., Le, S., Levy, B., Peinovich, M., Hanson, S., Passage, M., and Kakkis, E. (2007). Intrathecal enzyme replacement therapy: successful treatment of brain disease via the cerebrospinal fluid. Mol. Genet. Metab. *91*, 61–68.
33. Vite, C.H., Wang, P., Patel, R.T., Walton, R.M., Walkley, S.U., Sellers, R.S., Ellinwood, N.M., Cheng, A.S., White, J.T., O'Neill, C.A., and Haskins, M. (2011). Biodistribution and pharmacodynamics of recombinant human alpha-L-iduronidase (rhIDU) in mucopolysaccharidosis type I-affected cats following multiple intrathecal administrations. Mol. Genet. Metab. *103*, 268–274.
34. Kan, S.H., Aoyagi-Scharber, M., Le, S.Q., Vincelette, J., Ohmi, K., Bullens, S., Wendt, D.J., Christianson, T.M., Tiger, P.M., Brown, J.R., et al. (2014). Delivery of an enzyme-IGFII fusion protein to the mouse brain is therapeutic for mucopolysaccharidosis type IIIB. Proc. Natl. Acad. Sci. USA *111*, 14870–14875.
35. Aoyagi-Scharber, M., Crippen-Harmon, D., Lawrence, R., Vincelette, J., Yogalingam, G., Prill, H., Yip, B.K., Baridon, B., Vitelli, C., Lee, A., et al. (2017). Clearance of heparan sulfate and attenuation of CNS pathology by intracerebroventricular BMN 250 in Sanfilippo type B mice. Mol. Ther. Methods Clin. Dev. *6*, 43–53.
36. Boelens, J.J., Wynn, R.F., O'Meara, A., Veys, P., Bertrand, Y., Souillet, G., Wraith, J.E., Fischer, A., Cavazzana-Calvo, M., Sykora, K.W., et al. (2007). Outcomes of hematopoietic stem cell transplantation for Hurler's syndrome in Europe: a risk factor analysis for graft failure. Bone Marrow Transplant. *40*, 225–233.
37. Boelens, J.J., Rocha, V., Aldenhoven, M., Wynn, R., O'Meara, A., Michel, G., Ionescu, I., Parikh, S., Prasad, V.K., Szabolcs, P., et al.; EUROCORD, Inborn Error Working Party of EBMT and Duke University (2009). Risk factor analysis of outcomes after unrelated cord blood transplantation in patients with hurler syndrome. Biol. Blood Marrow Transplant. *15*, 618–625.
38. Watson, H.A., Holley, R.J., Langford-Smith, K.J., Wilkinson, F.L., van Kuppevelt, T.H., Wynn, R.F., Wraith, J.E., Merry, C.L., and Bigger, B.W. (2014). Heparan sulfate inhibits hematopoietic stem and progenitor cell migration and engraftment in mucopolysaccharidosis I. J. Biol. Chem. *289*, 36194–36203.
39. Wolf, D.A., Banerjee, S., Hackett, P.B., Whitley, C.B., McIvor, R.S., and Low, W.C. (2015). Gene therapy for neurologic manifestations of mucopolysaccharidoses. Expert Opin. Drug Deliv. *12*, 283–296.
40. Hinderer, C., Katz, N., Louboutin, J.P., Bell, P., Yu, H., Nayal, M., Kozarsky, K., O'Brien, W.T., Goode, T., and Wilson, J.M. (2016). Delivery of an adeno-associated virus vector into cerebrospinal fluid attenuates central nervous system disease in mucopolysaccharidosis Type II mice. Hum. Gene Ther. *27*, 906–915.
41. Stanford, K.I., Bishop, J.R., Foley, E.M., Gonzales, J.C., Niesman, I.R., Witztum, J.L., and Esko, J.D. (2009). Syndecan-1 is the primary heparan sulfate proteoglycan mediating hepatic clearance of triglyceride-rich lipoproteins in mice. J. Clin. Invest. *119*, 3236–3245.
42. Christianson, H.C., and Belting, M. (2014). Heparan sulfate proteoglycan as a cell-surface endocytosis receptor. Matrix Biol. *35*, 51–55.
43. Sarrazin, S., Lamanna, W.C., and Esko, J.D. (2011). Heparan sulfate proteoglycans. Cold Spring Harb. Perspect. Biol. *3*, a004952.
44. Orii, K.O., Grubb, J.H., Vogler, C., Levy, B., Tan, Y., Markova, K., Davidson, B.L., Mao, Q., Orii, T., Kondo, N., and Sly, W.S. (2005). Defining the pathway for Tat-mediated delivery of beta-glucuronidase in cultured cells and MPS VII mice. Mol. Ther. *12*, 345–352.
45. Xia, H., Mao, Q., and Davidson, B.L. (2001). The HIV Tat protein transduction domain improves the biodistribution of beta-glucuronidase expressed from recombinant viral vectors. Nat. Biotechnol. *19*, 640–644.
46. Dhuria, S.V., Hanson, L.R., and Frey, W.H., 2nd (2010). Intranasal delivery to the central nervous system: mechanisms and experimental considerations. J. Pharm. Sci. *99*, 1654–1673.
47. Djupesland, P.G., Messina, J.C., and Mahmoud, R.A. (2014). The nasal approach to delivering treatment for brain diseases: an anatomic, physiologic, and delivery technology overview. Ther. Deliv. *5*, 709–733.
48. Hamill, K.M., Wexselblatt, E., Tong, W.Y., Esko, J.D., and Tor, Y. (2016). Delivery of an active lysosomal enzyme using GNeosomes. J. Mater. Chem. B Mater. Biol. Med. *4*, 5794–5797.
49. Wexselblatt, E., Esko, J.D., and Tor, Y. (2015). GNeosomes: highly lysosomotropic nanoassemblies for lysosomal delivery. ACS Nano *9*, 3961–3968.

50. Fraldi, A., Klein, A.D., Medina, D.L., and Settembre, C. (2016). Brain disorders due to lysosomal dysfunction. Annu. Rev. Neurosci. *39*, 277–295.

51. Lamanna, W.C., Lawrence, R., Sarrazin, S., Lameda-Diaz, C., Gordts, P.L., Moremen, K.W., and Esko, J.D. (2012). A genetic model of substrate reduction therapy for mucopolysaccharidosis. J. Biol. Chem. *287*, 36283–36290.

52. Scudder, S.L., Goo, M.S., Cartier, A.E., Molteni, A., Schwarz, L.A., Wright, R., and Patrick, G.N. (2014). Synaptic strength is bidirectionally controlled by opposing activity-dependent regulation of Nedd4-1 and USP8. J. Neurosci. *34*, 16637–16649.

53. Esko, J.D. (1993). Special considerations for proteoglycans and glycosaminoglycans and their purification. In Current Protocols in Molecular Biology, F.M. Ausubel, R. Brent, R.E. Kingston, D.D. Moore, J.G. Seidman, and K. Struhl, eds. (Greene Publishing and Wiley-Interscience), pp. 17.2.1–17.2.9.

54. Esko, J.D., and Manzi, A. (1996). Measurement of uronic acids. In Current Protocols in Molecular Biology, F.M. Ausubel, R. Brent, R.E. Kingston, D.D. Moore, J.G. Seidman, and K. Struhl, eds. (Greene Publishing and Wiley-Interscience), pp. 17.19.8–17.19.11.